Available online at www.sciencedirect.com
SCIENCE DIRECT®
Physica C 412–414 (2004) 1484–1490
PHYSICA C
www.elsevier.com/locate/physc

Detection of deep-lying defects in carbon fiber composites using SQUID-NDE system cooled by a cryocooler

Y. Hatsukade [a,*], T. Inaba [a], N. Kasai [b], Y. Maruno [c], A. Ishiyama [d], S. Tanaka [a]

[a] *Toyohashi University of Technology, 1-1 Hibarigaoka, Tempaku-cho, Toyohashi, Aichi 441-8580, Japan*
[b] *National Institute of Advanced Industrial Science and Technology, AIST Tsukuba Central 2, Tsukuba, Ibaraki 305-8568, Japan*
[c] *Iwatani Industrial Gases Corporation, 4-5-1 Katsube, Moriyama, Shiga 524-0041, Japan*
[d] *Waseda University, 3-4-1 Ohkubo, Shinjuku, Tokyo 169-8555, Japan*

Received 29 October 2003; accepted 13 January 2004
Available online 1 June 2004

Abstract

In this paper, we present our latest progress in the studies on SQUID-NDE for carbon fiber composites (CFCs), including carbon fiber reinforced plastics (CFRPs) and carbon fiber reinforced carbon matrix composites (C/Cs). We have developed a new SQUID-NDE system for the CFCs utilizing a pulse tube cryocooler for more practical and easy-handling use. Electromagnets using U-shaped ferrite cores have been introduced to the system in order to induce enough eddy current density in the relatively low-electric-conductivity CFCs. By using this system, we demonstrated the detection of deep-lying defects in thick and/or multi-layer CFCs specimens, partly including metal layer upon/below CFCs layer. CFRP plates and multi-layer C/C plates with total thickness of 20 mm having deep-lying slots at various depths were prepared. The slots at 15 mm below the surface in the CFRP plate and multi-layer C/C plate were successfully detected. Defect detections on more "real" multi-layer structures, including aluminum plates upon/below C/C plates, were also examined.

PACS: 85.25; 81.70
Keywords: SQUID-NDE; Carbon fiber composites; Thick and multi-layer structures; Cryocooler

1. Introduction

In recent years, carbon fiber composites (CFCs), including carbon fiber reinforced plastics (CFRPs) and carbon fiber reinforced carbon matrix composites (C/Cs), have been preferably employed in several aerospace industries [1,2]. This is mainly due to the advantages of the composites, such as lightweight, high strength and stiffness. In addition, high-fatigue resistance, fracture toughness, and heat resistance up to 3000 K are the important advantages of C/Cs for high-temperature applications, like refractory tiles and nozzles

* Corresponding author. Tel.: +81-532-47-0111x5834; fax: +81-532-44-6926.
E-mail address: hatukade@eco.tut.ac.jp (Y. Hatsukade).

0921-4534/$ - see front matter © 2004 Elsevier B.V. All rights reserved.
doi:10.1016/j.physc.2004.01.145

of space shuttles [2,3]. However, the traditional NDE techniques, using ultrasonic, X-ray and acoustic emission, have faced serious difficulties in NDE on the CFCs, especially on C/Cs, due to their unique properties [4–6]. Furthermore, NDE on thick and/or multi-layered CFCs structures are almost impossible. This is the reason why the CFCs are rarely used in primary structures, which require high reliability. Because of these problems, we cannot fully take advantage of the CFCs.

From late '90, study on SQUID-NDE techniques for CFRPs was started [7]. So far, the effectiveness of the SQUID-NDE for relatively thin CFRP plates (a few mm thickness) has been revealed by some researches [8–10]. On the other hand, studies on SQUID-NDE for thick CFC materials, and for C/Cs have been also in progress [11–13]. Recently, we have improved our SQUID-NDE system by utilizing a coaxial pulse tube cryocooler (PTC) [13], while employing a high-T_c SQUID gradiometer and electromagnets with U-shaped ferrite cores [11], for more practical and easy-handling use in unshielded environments. By this system, defect detections on thick and/or multi-layer CFCs structures and even more "real" multi-layer structures, in which CFCs layers are combined with metal layers, should be possible.

By using the SQUID-NDE system, we demonstrated the detection of deep-lying defects in thick and/or multi-layer CFCs specimens, partly including metal layer upon/below CFCs layer. One-layer CFRP plates and multi-layer C/C plates with total thickness of 20 mm having deep-lying slots at various depths were prepared as specimens. These slots were inspected by the system. Inspection on the multi-layer C/C-Al specimens was also investigated.

2. Specimens

One-layer CFRP plates, multi-layer C/C plates, and multi-layer C/C-Al plates, with artificial deep-lying slots at various depths, were prepared as specimens.

The one-layer CFRP plates were made from cross-woven carbon fiber textures and polymer resin. The CFRPs plates were the laminated two-dimensional (2D) type. The fiber volume factor was 60%. The size of the CFRP plates was 200 mm in length, 250 mm in width and 20 mm in thickness. One CFRP plate had two slots with different depths D on back surface; D is the distance between surface and the top of the slot. Fig. 1(a) shows the cross-section of one CFRP plate. The

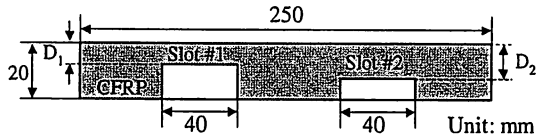

CFRP plates	Depth of slot #1	Depth of slot #2
No. 1	5 mm	17.5 mm
No. 2	7.5 mm	15 mm
No. 3	10 mm	12.5 mm

(a)

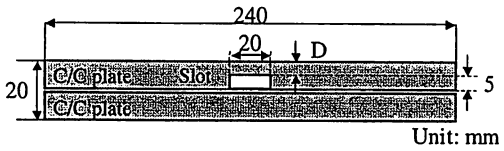

Multi-layer C/C	Depth of slot
Slot #1	0 mm
Slot #2	5 mm
Slot #3	10 mm
slot #4	15 mm

(b)

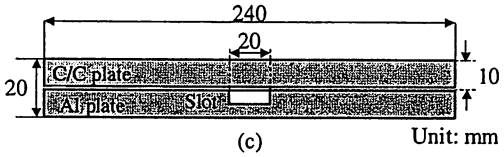

(c)

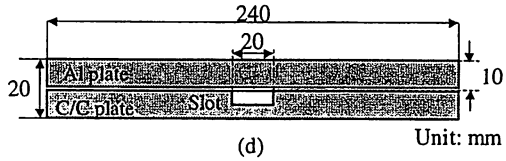

(d)

Fig. 1. Cross-sections of the prepared CFCs specimens. (a) One-layer CFRP plate with a pair of slots with different depths. (b) Multi-layer C/C specimen with slot. (c) Multi-layer (C/C)/Al specimen with slot of 10 mm depth. (d) Multi-layer Al/(C/C) specimen with slot of 10 mm depth.

depths of the pair slots D_1 and D_2 were 5 and 17.5 mm, 7.5 and 15 mm, and 10 and 12.5 mm, as shown in table in Fig. 1(a). The length and the width of the slots were 1 and 40 mm, respectively.

C/C plates composing the multi-layer C/C specimens were the cross-ply laminated 2D type with symmetric fiber orientation $[0/90/45/-45]_s$. The fiber volume factor was 50%. Pair of C/Cs plates was stacked as a multi-layer C/C specimen. Size of the specimens was 136 mm in length, 240 mm in width and 20 mm in thickness. Each specimen had a common-size slot of 2 mm in length, 20 mm in width and 5 mm in depth at different depth. Fig. 1(b) shows the cross-section of one multi-layer C/C specimen. The depths of the slots D were 0, 5, 10 and 15 mm, as shown in Table in Fig. 1(b).

Two types of the multi-layer C/C-Al specimens were prepared; one was a C/C plate stacked on an Al plate with a slot, and the other was an Al plate stacked on a C/C plate with a slot. The same C/C plates as the multi-layer C/C specimens were used. The sizes of the specimens and the slots were also same as those of the multi-layer C/C specimens. Fig. 1(c) and (d) show the cross-sections of the multi-layer (C/C)/Al specimen and the multi-layer Al/(C/C) specimen. Both specimens had single slot of 10 mm depth.

3. SQUID-NDE system cooled by a PTC

We have developed a SQUID-NDE system cooled by a coaxial PTC. This system is composed of a high-T_c SQUID gradiometer, SQUID electronics and non-magnetic cryostat, lock-in amplifier and current supplier, 2D scanning stage, the field generator using electromagnets, and the coaxial PTC with the compressor and the rotary valve. In this system, we employed a directly coupled type high-T_c SQUID gradiometer with differential pick-up coil, which was composed of two rectangular coils with size of 3.5 mm × 1 mm. The baseline length of the gradiometer was 3.5 mm. The field gradient sensitivity of the gradiometer was about 1.3 nT/m/Hz$^{1/2}$ at 100 Hz. The details of the system and the SQUID gradiometer were stated in elsewhere [13].

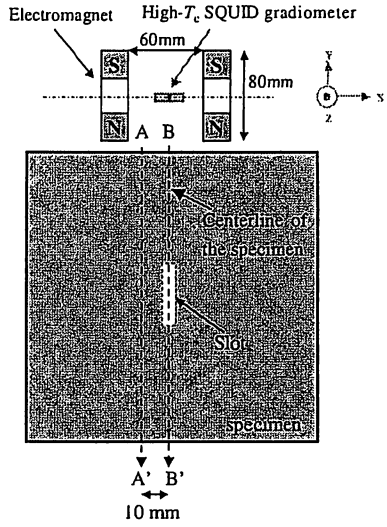

Fig. 2. System set up and the coordinates of the NDE measurements on the CFCs specimens. The line BB′ corresponds to the centerline of the specimens, where the slots exist along this line.

The magnetic field generator composed of a pair of U-shaped ferrite cores with permeability of 2300 μ_0 and 400-turn coils was employed to induce eddy current in the CFCs [11]. Distribution of the magnetic field generated by one U-shaped electromagnet resembles to that by a double-D coil [14]. Two electromagnets were fixed in parallel at both sides of the SQUID to keep symmetry of the generated field as shown in Fig. 2. The field generator generates ac magnetic field of 0.5 mT at a point 10 mm straight away from the core end with current of 100 mA. The frequency dependence of the generated field is roughly flat in the frequency range between 4 and 400 Hz. Alignments of two electromagnets are carefully adjusted by using the position-adjustment jig, in order to minimize the magnetic flux coupled to the SQUID from the electromagnets, before NDE measurements.

4. NDE measurements

The system set up and coordinates of NDE measurements on the specimens is schematically illustrated in Fig. 2. In all measurements, the following parameters are common; the distance

Table 1
The parameters used in NDE measurements

Specimen	Current supplied to EMs	Used SQUID	Measured component
CFRPs	200 mA at 310 Hz	Gradiometer	dB_z/dx
Multi-layer C/Cs	5 mA at 310 Hz	Gradiometer	dB_z/dx
(C/C)/Al	5 mA at 310 Hz	Magnetometer	B_z
Al/(C/C)	5 mA at 50 Hz, and 150 Hz	Magnetometer	B_z

between the high-T_c SQUID gradiometer and the surface of the specimen: 7 mm, the distance between core ends and the surface of the specimen: 3 mm, sampling space interval: 2 mm and measured component by the SQUID gradiometer: dB_z/dx. The SQUID was cooled at 75 K, and the cooling temperature was kept with thermal fluctuation of ±0.05 K during the measurements. 1D scanning and 2D scanning were properly carried out above the specimens. With some accidents, when the high-T_c SQUID gradiometer could not be operated, we properly employed a high-T_c SQUID magnetometer with field sensitivity of about 800 $\mu\Phi_0/\mathrm{Hz}^{1/2}$ at 100 Hz, instead of the gradiometer. The parameters used in the NDE measurements are summarized in Table 1.

5. Results and discussions

Results of the NDE measurements on one-layer CFRP plates obtained from 1D-scanning on the line AA′ in Fig. 2 are shown in Fig. 3(a). In the figure, the waveforms of the amplitude of magnetic field gradient are shown, together with the cross-section of the specimens on the line BB′ in Fig. 2. In all waveforms, each slot caused a pair of signal peaks above both sides of the slot. These pair peaks were confirmed to be the parts of quadratic signal peak due to the slot from 2D scanning around the slot. The deepest slot at 15 mm depth was also successfully detected. The signal peak amplitude decreases exponentially with the increase in the slot depth as shown in Fig. 3(b). According to the relation between the peak amplitude and the slot depth and the system noise shown in Fig. 3(b), more deep-lying slot located at about 30 mm should be detectable, where conventional NDE techniques should fail.

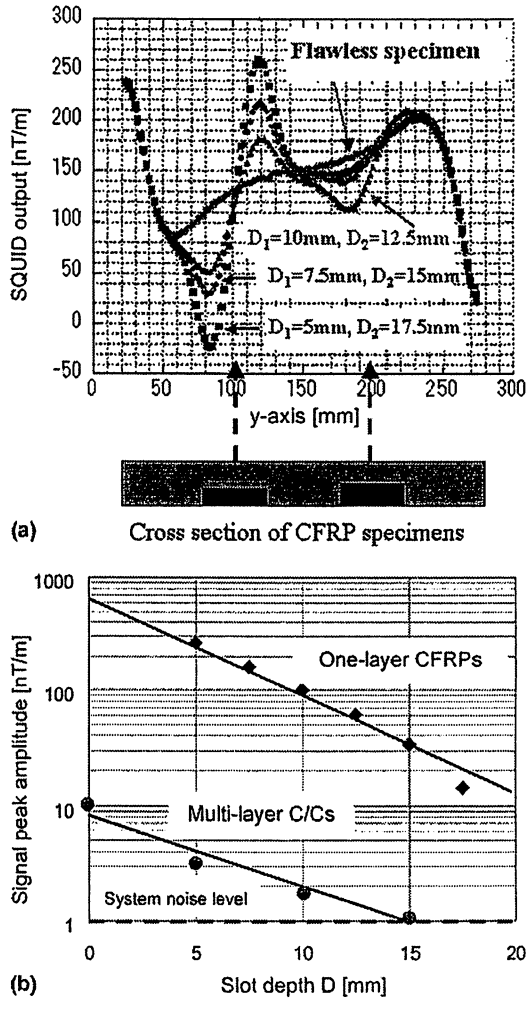

Fig. 3. Measurement results on one-layer CFRP plates. (a) Waveforms of magnetic field gradient. The cross-section of the specimen is illustrated below the waveforms. Pair of signal peaks appears above both sides of the slot. Waveform obtained from flawless same-size CFRP plate is drawn together for reference. (b) The relation between signal peak amplitude due to the slot and the slot depth. Results of both one-layer CFRPs and multi-layer C/Cs are drawn together.

The results on multi-layer C/C specimen obtained from 1D-scanning on the line AA′ in Fig. 2 are shown in Fig. 4. Same kind of the waveform as the results on one-layer CFRPs, in which signal peaks appeared above both sides of the slot, were obtained. Up to the deepest slot with $D = 15$ mm, all slots were detected. The relation between the signal peak amplitude and the slot depth is shown also in Fig. 3(b) with that of one-layer CFRPs. The exponential factor of the decrease in the peak amplitude of multi-layer C/Cs was approximately same as that of the one-layer CFRPs. It suggests that the ability of SQUID-NDE is independent on whether the specimen is stacked-type or not. The difference in the peak amplitude between multi-layer C/Cs and one-layer CFRPs are due to the difference in the current supplied into the field generator, 5 and 200 mA, respectively.

The measurement result of the slot in the multi-layer (C/C)/Al specimen is shown in Fig. 5(a), obtained by 1D-scanning on the line BB′ in Fig. 2. Since we used a high-T_c SQUID magnetometer in this case, the peaks of the signal due to the slot were measured on the line BB′, not on AA′. Because the electric conductivity of Al is much higher than that of C/Cs, the signal amplitude due to this slot is much stronger than that due to the same depth slot in multi-layer C/Cs. On the other hand, detection of the slot in multi-layer Al/(C/C) specimen was another story. Because of the upper Al plate with 10 mm thickness, lower frequency than 76 Hz (skin depth $\delta_{Al} = 10$ mm in Al) should be used to have the excitation field penetrate into the lower C/C plate. Then we applied excitation field at 50 Hz ($\delta_{Al} = 12$ mm) to the specimen. In this case, however, the signal peak due to the slot was superposed by large magnetic field due to the edge effect of Al plate. Therefore, we extracted the signal peak by means of applying the excitation filed at 150 Hz ($\delta_{Al} = 6.8$ mm) to the specimen in turn, then subtracting the measured data by 150 Hz from that by 50 Hz. The subtracted waveform of the magnetic flux obtained by 1D scanning on the line BB′ in Fig. 2 is drawn in Fig. 5(b). A pair of small signal peaks due to the slot in second-layer C/Cs was detected, while the edge effects remained still above both edges. The remaining of the edge effect is due to the difference between δ_{Al} at 50 and at 150 Hz. Problem of the edge effect must be solved for practical use.

From these results, it is clarified that SQUID-NDE have large advantage in defect detections on thick and/or multi-layer CFCs structures, including metal layers, compared to conventional NDE techniques. Furthermore, multi-frequency detection method used in this study should have a potential of the NDE on more "real", complicated CFCs structures, such as engine turbines, multi-layer wings, and surface-coated structures in aerospace applications [1–3].

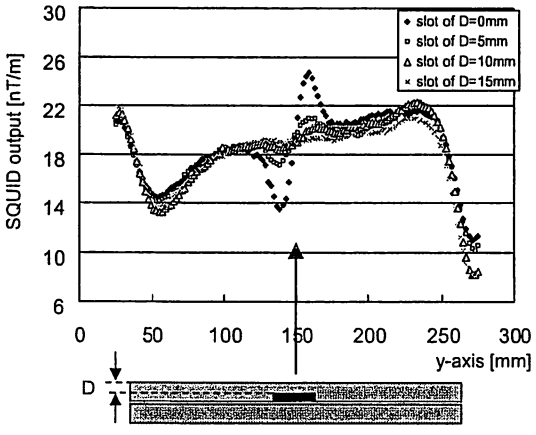

Fig. 4. Waveforms of magnetic field gradient obtained from C/C multi-layered specimens. The cross-section of the specimen is also illustrated below the waveforms.

6. Summary

We demonstrated the detection of deep-lying defects in the CFCs, including thick CFRPs, multi-layer C/Cs, and multi-layer (C/C)—Al structures. By using the SQUID-NDE system utilizing a PTC and electromagnets with U-shaped ferrite cores, the slots at least 15 mm depth in both CFRP and C/C multi-layer specimens were successfully detected. From these results, the slot at 30 mm depth should be detectable by means of coil current of 200 mA. Defect detection in multi-layer (C/C)—Al specimen was also examined while using two excitation frequencies, 50 and 150 Hz. The slot at 10 mm depth in second-layer C/Cs was detected by

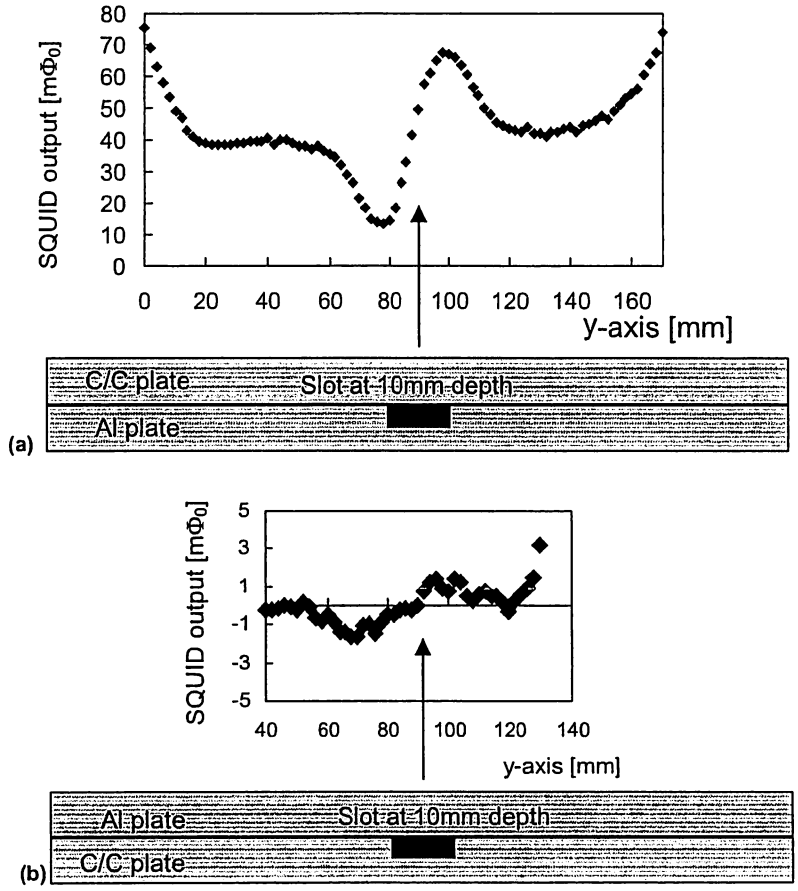

Fig. 5. Results of multi-layer (C/C)—Al specimens. (a) Waveform of magnetic flux obtained from (C/C)/Al specimen. (b) Waveform of magnetic flux obtained from Al on C/C specimen. The waveform was obtained by subtracting the data by using excitation frequency 150 Hz from that by 50 Hz.

subtracting the data obtained by 150 Hz from that by 50 Hz. These results suggest that defect detection in thick and complicated multi-layer structures using CFCs will be possible by using SQUID-NDE techniques.

Acknowledgements

We would like to acknowledge Professor Hatta of Institude of Space and Astronautical Science (ISAS) for offering us the C/Cs specimens.

References

[1] L.B. Ilcewicz, D.J. Hoffman, A.J. Fawcett, Comprehensive Composite Materials, Elsevier Science, Amsterdam, The Netherlands, 2000.
[2] J.D. Buckley, D.D. Edie, NASA Reference Publication 1254 (1992).
[3] D.L. Schmitdt, K.E. Davidson, L.S. Theibert, SAMPE J. 35 (1999) 27.
[4] Y.Z. Pappas, Y.P. Markopoulos, V. Kostopoulos, NDT & E Int. 31 (1998) 157.
[5] P.M. Deppech, D.M. Boscher, F. Lepoutre, A.A. Deom, D.L. Balageas, NDT & E Int. 29 (1996) 395.
[6] L. Dobiaova, V. Stary, P. Glogar, V. Valvoda, Carbon 40 (2002) 1419.

[7] N. Kasai, D. Suzuki, H. Takashima, M. Koyanagi, Y. Hatsukade, IEEE Trans. Appl. Supercond. 9 (1999) 4393.
[8] Y. Hatsukade, N. Kasai, A. Ishiyama, Jpn. J. Appl. 40 (2001) 606.
[9] A. Ruosi, M. Valentino, G. Peluso, G. Pepe, IEEE Trans. Appl. Supercond. 11 (2001) 1172.
[10] C. Carr, D. Graham, J.C. Macfarlane, G.B. Donaldson, IEEE Trans. Appl. Supercond. 13 (2003) 196.
[11] Y. Hatsukade, N. Kasai, H. Takashima, A. Ishiyama, Supercond. Sci. Technol. 15 (2002) 1728.
[12] Y. Hatsukade, M.S. Aly-Hassan, N. Kasai, H. Takashima, H. Hatta, A. Ishiyama, IEEE Trans. Appl. Supercond. 13 (2003) 207.
[13] Y. Hatsukade, N. Kasai, H. Takashima, A. Sakamaki, Y. Maruno, S. Tanaka, A. Ishiyama, Low-noise Cryocooler-cooled Compact SQUID-NDE System for Carbon-Fiber Composites, IOP Press (EUCAS2003), to be published in the Proceedings of EUCAS 2003 (IOP), 2004.
[14] A. Ruosi, G. Pepe, G. Peluso, M. Valentino, M. Monebhurrun, IEEE Trans. Appl. Supercond. 9 (1999) 3499.